Accepted Manuscript

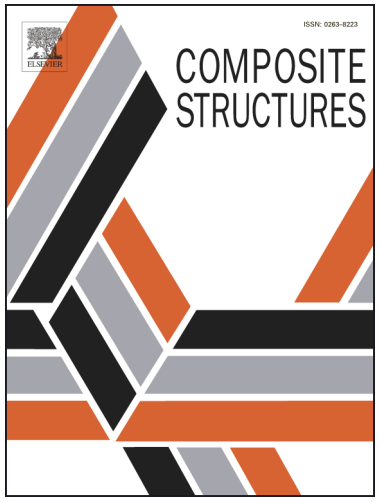

Non-Contact Magnetic Driving Bioinspired Venus Flytrap Robot Based On Bi-stable Anti-symmetric CFRP Structure

Zheng Zhang, Dandi Chen, Huaping Wu, Yumei Bao, Guozhong Chai

PII: S0263-8223(15)00851-X
DOI: http://dx.doi.org/10.1016/j.compstruct.2015.09.015
Reference: COST 6860

To appear in: *Composite Structures*

Please cite this article as: Zhang, Z., Chen, D., Wu, H., Bao, Y., Chai, G., Non-Contact Magnetic Driving Bioinspired Venus Flytrap Robot Based On Bistable Anti-symmetric CFRP Structure, *Composite Structures* (2015), doi: http://dx.doi.org/10.1016/j.compstruct.2015.09.015

Non-Contact Magnetic Driving Bioinspired Venus Flytrap Robot Based On Bistable Anti-symmetric CFRP Structure

Zheng Zhang[a,b]*, Dandi Chen[a], Huaping Wu[a], Yumei Bao[a], Guozhong Chai[a]

[a]Key Laboratory of E&M (Zhejiang University of Technology), Ministry of Education & Zhejiang Province, Hangzhou 310014, P.R. China

[b]School of Civil Engineering, The University of Queensland, St Lucia, QLD 4072, Australia

*Corresponding author. E-mail address: zzhangme@zjut.edu.cn (Zheng Zhang), Telephone: 86-571-88320244.

Abstract: The Venus flytrap takes advantage of its bistability to generate rapid closure motion for capturing its prey. A bioinspired Venus flytrap robot with bistable artifical leaves is presented in this paper. Non-contact electromagnetic driving method is proposed to actuate the Venus flytrap robot's artifical leaves, which are made of anti-symmetric carbon fiber reinforced prepreg (CFRP) cylindrical shells. Magnetic force is generated by using the electromagnet and applied on the shell's curve edge to unbend the shell, and then the bending process transmits from one edge to the whole surface. The required magnetic force for the snap-through process of the bistable CFRP structure is determined from experimental test and compared with the result of finite element simulation. The test of the snap-through process of the Venus flytrap robot show that the Venus flytrap robot can generate a rapid snapping motion by the electromagnet actuation.

Keywords: bioinspired Venus flytrap; magnetic driving; bistable composite structure; anti-symmetric cylindrical shell; non-contact.

1. Introduction

In recent years, the bioinspired and biomimetic designs have become more

popular than ever for its comprehensive properties and potential engineering applications. The Venus flytrap, as an interesting insectivorous plant among these, has been attracting the attention of many researchers. When insects or small animals touch the trigger hair of the Venus flytrap, its two leaves can close rapidly to capture the prey, as shown in the Fig. 1.

The active trapping mechanism of Venus flytrap was first presented by Williams [1] and Jacobson [2]. Then a dynamic response model of the Venus flytrap was founded [3] and then a Venus flytrap robot, also known as robotic flytrap, based on the model by using ionic polymeric metal composite (IPMC) artificial muscles as sensors and actuators was designed by Shahinpoor [4]. A Venus flytrap robot by the means of two IPMC actuators and one proximity sensor is presented by Shi [5-6]. Both above two researchers regarded the capture process of Venus flytrap as a single active deformation process. According to Forterre's research [7], the morphing motion of the Venus flytrap is composed of two processes: one is an active biochemical process, and the other is a passive elastic deformation process. The active biochemical process is caused by a rapid loss of turgor pressure in 'motor cells' [8]. The reason for the passive elastic deformation process is the existence of the bistability of its special leaves which is induced by its geometric characteristic. Therefore, the Venus flytrap leaf is a bistable structure with two different stable states: opening state with leaves being flat and closing state with leaves being coiled. Based on this interesting characteristic of the Venus flytrap, some bioinspired Venus flytrap robots have been developed by the use of bistable composite structures. A Venus flytrap robot made from cross-ply bistable CFRP structures and actuated by shape memory alloy (SMA) springs was developed by Kim et al. [9-11]. The Venus flytrap robot is able to complete the shape transition process in a short time under the actuation of SMA springs, which is similar to the capture mechanism of real Venus flytrap. However, the cross-ply bistable CFRP structure has two contrary curvature directions in the interchange of two stable states [12], it doesn't exactly depict the real curvature change of the Venus flytrap. Therefore, the bistable anti-symmetric CFRP structure which has the same curvature direction at the two stable shapes [13] is chosen to act

as the artificial leaf in present paper to mimic the real Venus flytrap predation behaviour.

Due to the similar deformation mechanism between the bistable laminated CFRP stucture and the Venus flytrap's leaves, the bistable laminated CFRP structure is appropriate to be used to design a Venus flytrap robot. The bistable laminated CFRP structures were studied by researchers for its unique bistability [14-16]. In addition, it is widely used in smart structures and deployable structures with kinds of actuations [17-22]. Dano et al. [23], Schultz et al. [24] and Hufenbach et al. [25] used shape memory alloy (SMA) wires or macro fiber composites (MFCs) as the actuator to induce the snap-through action of cross-ply bistable CFRP structure. As references described above, these trigger forces applied to driving the cross-ply bistable CFRP are at a low intensity. The bistable anti-symmetric CFRP structure needs larger trigger force than cross-ply bistable CFRP structure so it is usually loaded only by mechanical forces in experiments [26-27].

In order to generate a proper trigger force for the bistable anti-symmetric CFRP structure, a kind of magnetic actuation is presented in this paper. It is well-known that magnetic force can be applied without contact and easily adjusted by changing the applied current when using an electromagnet. Magnetic actuations are widely used in some smart structures for these advantages. A penta-stable structure was designed by Zhao [28], utilizing the mechanical-magnetic coupling effects of five arranged permanent magnets. Nam [29] developed a micro crawling robot which was driven by external magnetic field. It can crawl through a tunnel freely by the friction generated from the magnetic force. Sendoh [30] used an adjustable magnetic field to acquire required magnetic force and moment to drive micro robot. A kind of microrobot prototype for force sensing was presented by Jing [31]. Because of the limitation of the usual actuation and the advantages of the electromagnet such as no-contact and adjustable characteristics, electromagnet driving method is chosen to act as the actuation of the bistable anti-symmetric CFRP structure.

Therefore, A Venus flytrap robot with its leaves made of bistable anti-symmetric CFRP structures and driven by an electromagnetic actuation is presented in this paper.

First, the basic principle of the artificial leaf made of bistable anti-symmetric CFRP shell and the new actuation method based on electromagnet are given. Subsequently, experimental tests and finite element analysis are conducted to determine the required magnetic force for the snap-through motion. The comparison of the experimental and numerical results is given. Finally, the capture motion of the Venus flytrap robot is performed successfully and the closure posture of Venus flytrap robot is achieved.

2. Venus Flytrap Robot's Design and Assembly

The schematic of a novel Venus flytrap robot, which can close rapidly like a real Venus flytrap, is shown in Fig. 2. In order to mimic the shape of the real leaf, the artificial leaf is made of bistable anti-symmetric CFRP structure which has two positive curvatures at its stable states. The deformation process can be triggered to snap through by an electromagnet. This section focuses on the design and assembly of the Venus flytrap robot. The corresponding capture motion is realized using the magnet actuator. In order to keep the artificial leaf close completely at the second stable state, the length and the layups of the bistable shell have to be designed to acquire the demand curvatures, which are discussed together with the actuation method in this section.

2.1 The artificial leaf

The anti-symmetric CFRP shell has two unique features compared with the real Venus flytrap's leaf: (a) The actual Venus flytrap leaves are doubly-curved leaves both in the opening and closing stable states, its curvature changes during the whole snap process. The anti-symmetric CFRP shell has a positive curvature in one direction and a zero curvature in the other direction at the initial stable state, the positive curvature turns to zero and the zero curvature turns to positive when it changes to the second stable state. (b) The deformation of both kinds of leaves from the initial stable state to the second stable state is induced by a trigger force. The difference is that the actuation in the actual Venus flytrap is induced by the internal 'motor cells' while the trigger force in the Venus flytrap robot is an external magnetic force.

It is important for the Venus flytrap to keep the insect from escaping. Therefore, the leaf of Venus flytrap should close completely and rapidly, so does the artificial leaf. For this purpose, proper bi-stable shells with particular geometric parameters should be selected. As also shown in Fig.2, the opening and closing states of the Venus flytrap are given. The geometric parameters of the Venus flytrap robot's first stable configuration (Fig.2(a)) are: L=100mm, R=25mm, γ=180°, thickness of lamina t=0.12mm and the layup is [45°/-45°/45°/-45°]. According to the finite element analysis of different geometrical parameters at the first stable state, the results show that the artificial leaf of the Venus flytrap robot with this dimension can close completely at the second stable state. Subsequently, the bistable anti-symmetric CFRP shells were manufactured using a cylindrical steel mold with a pre-load on the upper part using carbon-fiber/epoxy prepreg. The material properties of the used shell are listed in Table 1. The bistable anti-symmetric CFRP shells' specimens are testified to have a good performance in bistablity and the deformation processes agree well with the numerical results. The closing state of the leaf at the second stable state, shown in the Fig. 2(b), depends on the geometric parameters at the first stable state and the material properties [26-27]. Therefore, the selected artificial leaf can close completely at the second stable state by adjusting the geometric parameters of the first stable state before specimen manufacturing.

2.2 Triggering actuation

The capture motion of the bistable CFRP structure is divided into two processes: triggering actuation and snap-through process. The snap-through process occurs automatically when the triggering actuation is completed. Thus, the triggering actuation is crucial to the snap-through process of the Venus flytrap robot.

The common characteristics used external force as actuators is that the first step is to unbend the bistable CFRP structure, and then its snap-through process is induced. Actuator arrangements of different unbending actuations are given in Fig.3. The red points denotes the actuation points. For common unbending actuation like SMA or MFCs (Fig.3(a)), the actuator is located on straight edge or along the center line. For

magnetic unbending actuation (Fig.3(b)), the actuator is located on the curve edge. Force or moment was applied to flatten the structure, and then the snap-through process occurs. The common actuations needs a larger supporter or several actuation patches to provide the trigger force. The larger supporter would make the structure more complicated and actuators along the curve should affect the stiffness of the whole structure. Moreover, most of the common actuations are applied on cross-ply bistable CFRP structure, whose required trigger force is lower than that of the bistable anti-symmetric CFRP structure. The common actuations are not suitable for the Venus flytrap robot with the bistable anti-symmetric CFRP structure leaves because most of the actuations couldn't afford enough trigger force for the bistable anti-symmetric CFRP structure.

The novel electromagnetic actuation here we introduce is different from the common actuations for the bistable CFRP shell. The unbending actuation applies the electromagnetic force with perpendicular curve direction, see the point A in Fig. 3(b). The center part of the opposite curve edge is fixed, shown as the area between point B and point C at the curve edge. When magnetic force is applied on the point A, a bending moment will generate at the fixed area between point B and point C. This unbending moment applied along the curve edge unbends the curve until it reaches the trigger position, where the snap-through process occurs. Then the shell turns to its second stable state rapidly.

As mentioned above, the magnetic force can be generated by non-contact method and adjusted by changing the current applied on the electromagnet. When the distance between the magnet and iron is close enough, it can generate a large magnetic force. But the magnetic force would become weak rapidly as the distance increases.

2.3 Assembly

The whole Venus flytrap robot prototype is composed of three parts: two artificial leaves made of anti-symmetric CFRP shells, a magnet bonded on each leaf and a supporter to hold the leaf. The middle part of the curve edge of the artificial leaf is fixed on the supporter with two bolts along the edge. The two artificial leaves are

mounted on the supporter symmetrically, just like the real Venus flytrap. The supporter is a flat plate made of ABS resin material. The opening and closing states of the Venus flytrap robot prototype are shown in Fig. 4.

The magnetic actuation is made of two parts: an electromagnet and an iron patch. The iron patch is fixed at the middle part of the other curve edge of the artificial leaf. In order to obtain a larger magnetic force, the iron patch is attached at the upper side of the leaf and the electromagnet is placed just above the iron patch. A DC power supply and some wires are used to activate the electromagnet. When the electromagnet is activated, it induces a magnetic force at the curve edge which generates bending moment on the bistable structure to drive the leaves deforming into the second stable state.

3. Experiment and Simulation

This section presents the experimental test and numerical simulation of the Venus flytrap robot. The required magnetic force is measured and the experimental result is compared with numerical results obtained from ABAQUS software. The relation of maximum magnetic force and the current applied on the electromagnet is obtained and the experimental result is compared with numerical results from ANSYS software. Finally, the snap-through process of Venus flytrap prototype is investigated.

3.1 Measurement of the trigger force

The experiment was designed to gain the loading force to trigger the snap-through process. The selected permanent magnet's component is Nd-Fe-B with a size of $20\times10\times4$mm and a 4mm diameter hole in the center for fixing. The number of magnets can be changed to adjust the magnetic force. More magnets mean a larger force. One of the magnets was fixed at the middle part of the curve edge of the artificial leaf. The other magnets were piled up as a magnet block. Then the magnet block was moved towards the single magnet, and the single magnet was attracted to the block. Then the snap-through process of the artificial leaf can be triggered. If the snap-through process is completed, the number of magnets in the block will reduce,

and the test will be repeated until the snap-through process failed. The magnet block at the next-to-last time is called as the 'trigger magnet block'. 5 magnets were used to induced the actuation firstly, when the number of the magnets was reduced to 2, the magnets couldn't induce the actuation of the structure at that time. Hence, the 'trigger magnet block' was made up of 3 magnets.

Then, the force between the trigger magnet block and the single magnet needed to be acquired. A simple experiment is designed for the measurement of magnetic force, as shown in Fig. 5, the single magnet was fixed at the downside of a plate with a bolt and the trigger magnet block was placed under the single magnet. A water container was hanged on the magnet block by nylon wire. Water as a load was gradually added to the bottle until the magnet block separated from the single magnet. Thus, the weight of the bottle and water inside was equal to the maximum value of the magnetic force between the magnet block and the single magnet, which was also approximate to the trigger force of the Venus flytrap robot. The trigger force is measured three times and the mean value is 41.46N.

Finite element model is used to simulate the bistable CFRP shell deformation process, shown in Fig. 6. The geometric parameters of first stable configuration are: L=100mm, R=25mm, γ=180°, thickness of lamina t=0.12mm and the layup is [45°/-45°/45°/-45°]. The material properties of the shell are listed in Table 1. Here S4R reduced integration shell element with a mesh density of 40×50 is chosen for simulation. The center part of one curve edge of the shell was constrained in "*Displacement/Rotation*" boundary conditions, as the leaf was assumed to be entirely fixed on the supporter. To simplify computational model, the trigger force generated by the single magnet was supposed to distribute evenly on the leaves. Therefore, at the other curve edge, a "Pressure" is applied at the same place where the single magnet is fixed. The option *Nlgeom* is selected in both steps. The value of the pressure is adjusted around the measured value 41.46N until the snap-through process is completed in ABAQUS software.

Two steps are included in the present finite element analysis: (1) *Pressure* is loaded in order to make the shell snapping from initial stable state to the second stable

state. (2) Remove the *pressure* and relax the shell until it reaches the second stable state.

The comparison of experimental and numerical results is shown in Fig. 7. The unbending process of the shell in the experiment and the simulation both occurred at the fixed place of the leaf at first, then it spreads to the whole shell. The radius of the leaf in the second stable state was measured by analyzing the configuration of the shell by digital image technology in MATLAB software. The experimental result of the radius at the second stable shape is 26.07 mm, while the numerical result is 35.09mm. The required trigger force measured in the experiment is 41.46N, whereas the finite element predicted trigger force is 50.1N. It is believed that the main reason of the difference between finite element predicted and measured forces is that there exists stricter constraint condition in the simulation and theoretical assumption in the ABAQUS model. As a result, the radius and trigger force of the finite element results are larger than that of experimental results.

3.2 Measurement of the magnetic force

To actuate the artificial leaf of Venus flytrap robot, the magnetic force generated by the electromagnet has to exceed the trigger force 41.46N of the snap-through process of the artificial leaf. The electromagnet was chosen and the measurement of trigger force by electromagnet was given in Fig. 8. In order to obtain the appropriate current, a simple testing method is introduced. It is similar to the method we used above to determine the trigger force of the artificial leaf. However, the current value is changed here. As the current reaches a certain value when the magnetic force is high enough to induce snap-through process, the minimum current is acquired. This measurement was repeated 3 times and the mean value is 0.18A.

At the same time, the magnetic force is acquired by using ANSYS software. The ANSYS model of the electromagnet is an axial symmetry 2D model, shown in the Fig. 9. The relative permeability of the iron core of the electromagnet and the iron attached to the artificial leaf is 700 from the manufacturer. The relative permeability of air and copper wire is 1. The element type of “Vect Quad 8node53” was chosen in free mesh

method by ANSYS software. As can be seen in Fig.9, the purple zone means the iron core, the red zone is the copper wire, and the light blue zone is the air and the dark blue zone denotes the attracted iron. The distance between the electromagnet and the attracted iron was supposed to be 0.1mm. The current was applied on the red zone by the average value of current (0.18A/the area of the red zone). The magnetic force generated by the electromagnet is turned out as 31.36N. The force of the electromagnet is significantly influenced by the distance between the electromagnet and the attracted iron patch. As the distance between electromagnet and the attracted iron is hard to measure, an estimated value according to the roughness of the iron is used in the finite element simulation, which might be the main reason to lead the difference between the numerical and experimental result.

3.3 Snap-through process of the Venus flytrap robot

The snap-through process of the Venus flytrap induced by the electromagnet actuation is shown in Fig. 10. As can be seen, the Venus flytrap prototype was closed completely. As the artificial leaf is a cylindrical shell, its straight edges turn to curve edges after snap-through process, which means the leaf cannot close completely at the both sides of the Venus flytrap robot. Some plastic sectors adhered to the edges of the artificial leaf are used to cover the blank part of the artificial leaf. When the Venus flytrap robot opens, these sectors are arrayed in parallel on the edge. In the closing state, these sectors form a circle lid to prevent insects inside from escaping, which have similar function to the jagged edges of the real Venus flytrap leaf.

The motion of the single leaf of Venus flytrap robot was recorded by a digital camera with 25fps recording rate. The triggering actuation took about 1.32s, but the snap-through time was about 0.2s. It is very similar to the capture process of real Venus flytrap, which also morphs slowly in the triggering process but closes rapidly in the snap-through process. The results also show the bi-stable anti-symmetric CFRP shell has the same magnitude of capture velocity with cross-ply CFRP shell driven by SMA [10].

4. Conclusions

In this paper, a bioinspired Venus flytrap robot with bistable artificial leaves and electromagnet actuation is presented to generate a rapid snapping motion. When the electromagnet is activated by appropriate current, the irons attached to the artificial leaves are attracted to the electromagnet. The leaf driven by the electromagnet moves to a particular position, and changes from initial stable state to second stable state rapidly. Subsequently, the magnetic force is removed and the artificial leaf remains at its second stable state. This is very similar to the capture motion of the real Venus flytrap. The magnetic force was measured and compared to the numerical results. The results show that the presented Venus flytrap robot combined with bistable characteristic and magnetic actuation, which has a rapid and large morphing motion without complex structures, is significant in many engineering fields such as small gripping device, scalable hinge, morphing wings and other deployable structures.

Acknowledgement

This research was supported by the National Natural Science Foundation of China (Grant No. 51205355, 11372280), the Zhejiang Provincial Natural Science Foundation of China (Grant No. LY15E050016), the Research Fund for the Doctoral Program of Higher Education of China (Grant No. 20123317120003), the Postdoctoral Science Foundation of China (Grant No. 2013M540498). The first author (Zheng Zhang) is grateful for the support provided by the China Scholarship Council (CSC) which enables him to conduct research at the University of Queensland.

References

[1] Williams M E, Mozingo H N. The fine structure of the trigger hair in Venus's flytrap. Am J Bot, 1971; 532-9.

[2] Jacobson S L. Effect of ionic environment on the response of the sensory hair of

Venus's-flytrap. Can J Bot, 1974; 52(6): 1293-302.

[3] Shahinpoor M, Thompson M S. The Venus Flytrap as a model for a biomimetic material with built-in sensors and actuators. Mat Sci Eng C-Mater, 1995; 2(4): 229-33.

[4] Shahinpoor M. Biomimetic robotic Venus flytrap (Dionaea muscipula Ellis) made with ionic polymer metal composites. Bioinspir Biomim, 2011; 6(4): 046004.

[5] Shi L, Guo S, Kudo H, et al. Development of a Venus flytrap-inspired robotic flytrap. Robotics and Biomimetics (ROBIO), 2012 IEEE International Conference on. IEEE, 2012: 551-6.

[6] Shi L, He Y, Guo S, et al. IPMC actuator-based a movable robotic venus flytrap. Complex Medical Engineering (CME), 2013 ICME International Conference on. IEEE, 2013: 375-8.

[7] Forterre Y, Skotheim JM, Dumais J, et al. How the Venus flytrap snaps. Nature, 2005; 433: 421-5.

[8] Hill BS, Findlay GP. The power of movement in plants: the role of osmotic machines. Q Rev Biophys, 1981;14:173-222.

[9] Kim S W, Koh J S, Cho M, et al. Towards a bio-mimetic flytrap robot based on a snap-through mechanism. Biomedical Robotics and Biomechatronics (BioRob), 2010 3rd IEEE RAS and EMBS International Conference on. IEEE, 2010: 534-9.

[10] Kim S W, Koh J S, Cho M, et al. Design & analysis a flytrap robot using bi-stable composite. Robotics and Automation (ICRA), 2011 IEEE International Conference on. IEEE, 2011: 215-220.

[11] Kim S W, Koh J S, Lee J G, et al. Flytrap-inspired robot using structurally integrated actuation based on bistability and a developable surface. Bioinspir Biomim, 2014; 9(3): 036004.

[12] Mattioni F, Weaver PM, Potter K, et al. The analysis of cool-down and snap-through of cross-ply laminates used as multistable structures. ABAQUS UK group conference, 2006.

[13] Hyer MW. The room-temperature shapes of four-layer unsymmetric cross-ply laminates. J Compos Mater, 1982; 16: 318-40.

[14] Giddings P F, Bowen C R, Salo A I T, et al. Bistable composite laminates: effects of laminate composition on cured shape and response to thermal load. Composite Struct, 2010; 92(9): 2220-5.

[15] Cantera, M. A., et al. Modelling and testing of the snap-through process of bi-stable cross-ply composites. Compos Struct, 2015; 120: 41-52.

[16] Kuder, Izabela K., Andres F., et al. Design space of embeddable variable stiffness bi-stable elements for morphing applications. Compos Struct, 2015; 122: 445-55.

[17] Daynes S., Weaver P. M., Review of shape-morphing automobile structures: concepts and outlook. P I Mech Eng D-J Aut. 2013; 227(11): 1603-22.

[18] Daynes S, Weaver PM, Potter KD. Aeroelastic Study of Bistable Composite Airfoils. J Aircraft, 2009; 46: 2169-74.

[19] Thill C., Etches J., Bond I., et al. Morphing skins. Aeronaut J, 2008; 112: 117-139.

[20] Lachenal X., Daynes S., Weaver P. M., Review of morphing concepts and materials for wind turbine blade applications. Wind Energy, 2013; 16: 293-307.

[21] Dai F, Li H, Du S. A multi-stable lattice structure and its snap-through behavior among multiple states. Compos Struct, 2013; 97: 56-63.

[22] Bowen CR, Butler R, Jervis R, Kim HA, Salo AIT. Morphing and Shape Control using Unsymmetrical Composites. J Intel Mat Syst Str, 2006; 18: 89-98.

[23] Dano M L, Hyer M W. SMA-induced snap-through of unsymmetric fiber-reinforced composite laminates Int. J. Solids Struct. 2003; 40: 5949–72.

[24] Schultz MR, Hyer MW. Snap-through of unsymmetric cross-ply laminates using piezoceramic actuators. J Intel Mat Syst Str, 2003; 14: 795-814.

[25] Hufenbach W, Gude M, Czulak A. Actor-initiated snap-through of unsymmetric composites with multiple deformation states. J Mater Process Tech, 2006; 175: 225-30.

[26] Zhang Z, Wu H, He X, Wu H, Bao Y, Chai G. The bistable behaviors of carbon-fiber/epoxy anti-symmetric composite shells. Compos Part B-Eng, 2013; 47: 190-9.

[27] Zhang Z, Wu H, Ye G, et al. Systematic experimental and numerical study of bistable snap processes for anti-symmetric cylindrical shells. Compos Struct, 2014; 112: 368-77.

[28] Zhao, Jian, et al. Mechanical-Magnetic Coupling Analysis of a Novel Large Stroke Penta-Stable Mechanism Possessing Multistability Transforming Capability. Journal of Mechanisms and Robotics, 2014; 6(3): 031004.

[29] Nam J, Jeon S, Kim S, et al. Crawling microrobot actuated by a magnetic navigation system in tubular environments. Sensor Actuat A-Phys, 2014; 209: 100-6.

[30] Sendoh M, Ishiyama K, Arai K I. Fabrication of magnetic actuator for use in a capsule endoscope. Magnetics, IEEE Transactions on, 2003; 39(5): 3232-4.

[31] Jing, Wuming, and David Cappelleri. A Magnetic Microrobot with in situ Force Sensing Capabilities. Robotics, 2014; 3(2): 106-19.

Fig. 1 Venus Flytrap in the nature.

Fig. 2 Two stable states of the Venus flytrap.

(a) Opening state;

(b) Closing state.

Fig. 3 Actuator arrangements of different unbending actuations.

(a) Process of common unbending actuation;

(b) Process of magnetic unbending actuation.

Fig. 4 Bioinspired Venus flytrap robot prototype.

(a) Opening state;

(b) Closing state.

Fig. 5 The measurement of the magnetic force.

Fig. 6 Model of the bi-stable CFRP shell in ABAQUS software.

Fig. 7 Deformation process of the bi-stable CFRP shell.

(a) In the experiment;

(b) In the ABAQUS simulation;

(1) Opening state; (2) Transforming state; (3) Closing state.

Fig. 8 Measurement of the trigger force by electromagnet.

Fig. 9 Axial symmetric 2D model of the electromagnet in ANSYS software.

Fig. 10 Venus flytrap robot with plastic sectors.

(a) Opening state;

(b) Closing state.

Table 1. The material properties of carbon-epoxy lamina

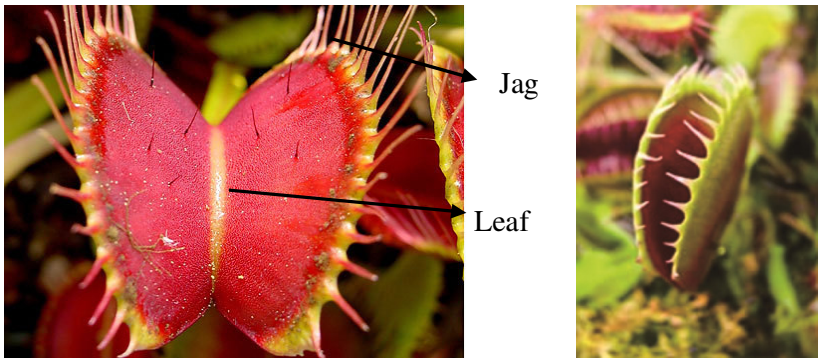

Fig. 1 Venus Flytrap in the nature.

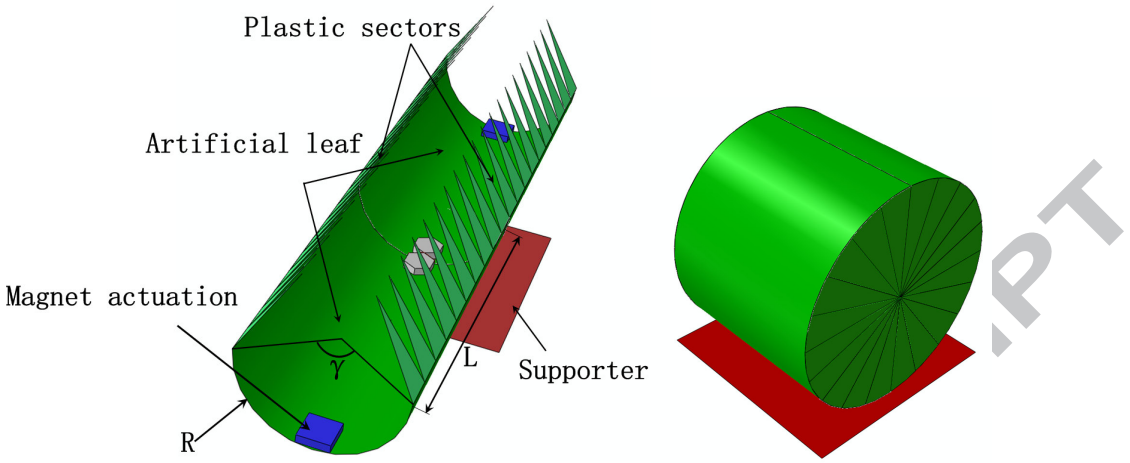

(a) (b)

Fig. 2 Two stable states of the Venus flytrap: (a) Opening state; (b) Closing state.

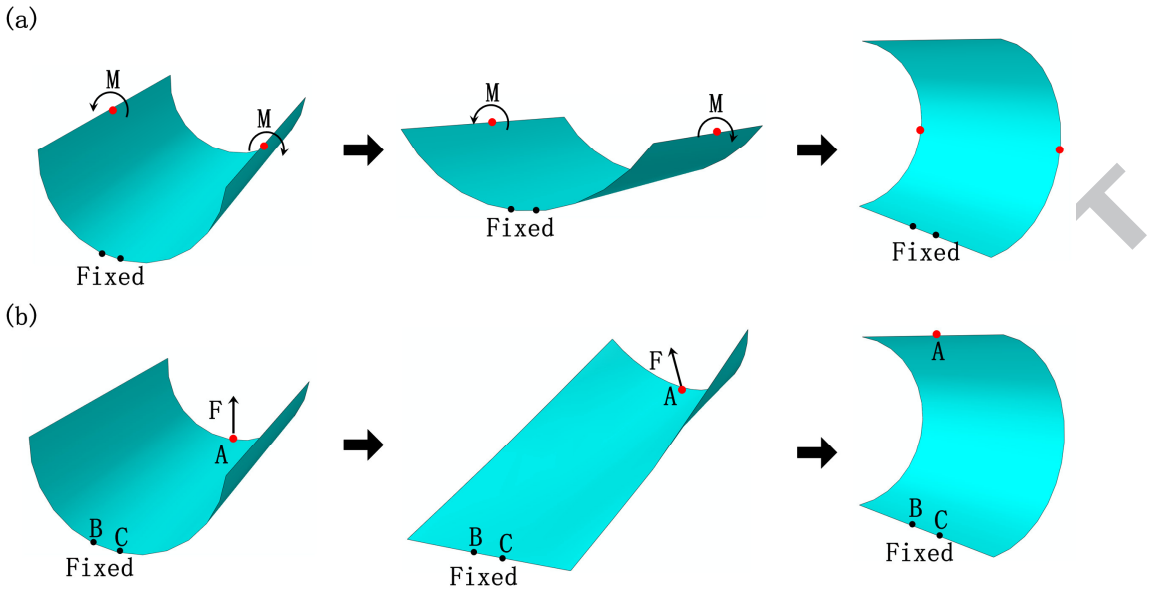

Fig. 3 Actuator arrangements of different unbending actuations: (a) Process of common unbending actuation; (b) Process of magnetic unbending actuation.

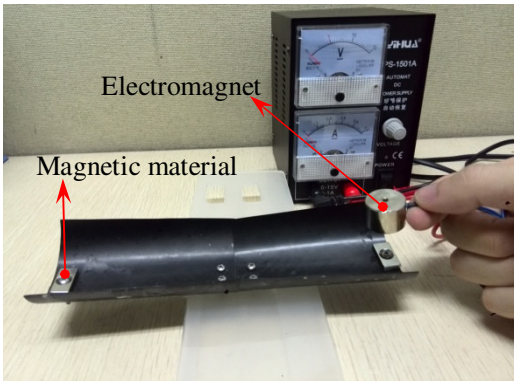

(a)

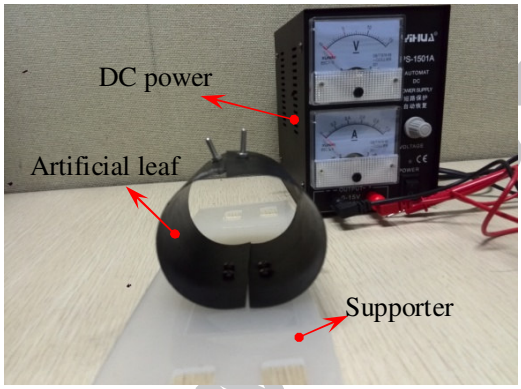

(b)

Fig. 4 Bioinspired flytrap robot prototype: (a) Opening state; (b) Closing state.

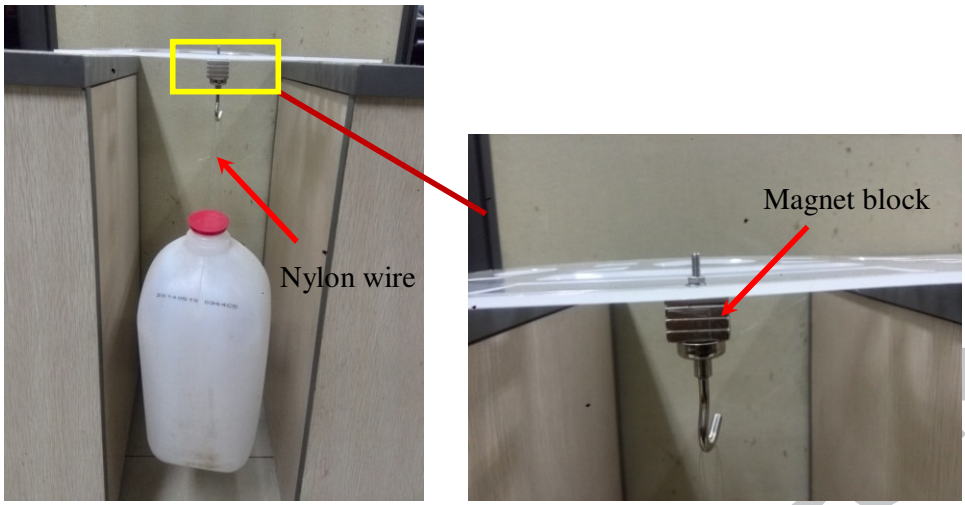

Fig. 5 The measurement of the magnetic force.

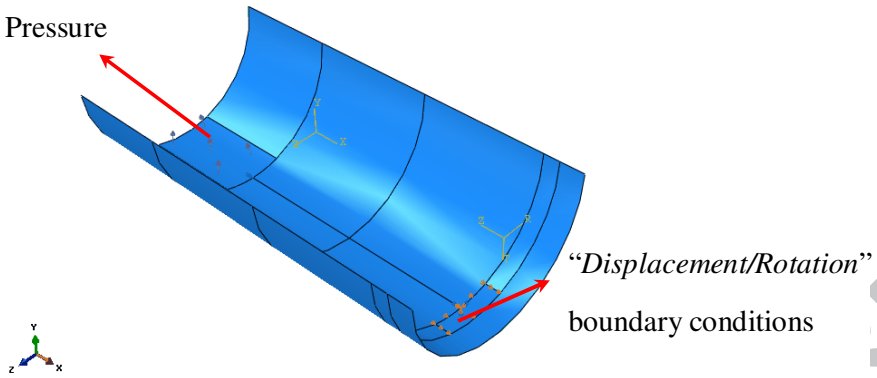

Fig. 6 Model of the bi-stable CFRP shell in ABAQUS software.

(a)

(1) (2) (3)

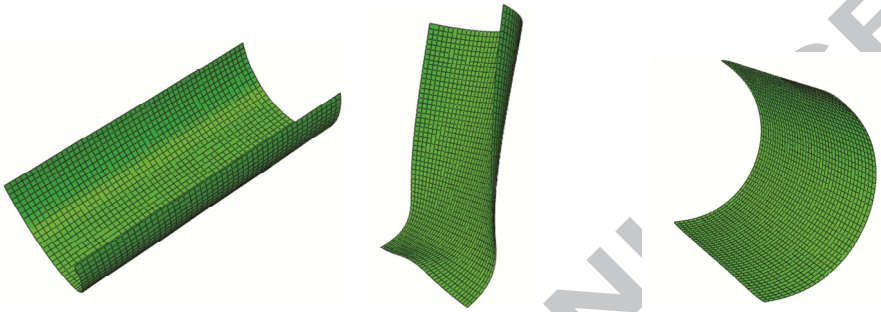

(b)

(1) (2) (3)

Fig. 7 Deformation process of the bi-stable CFRP shell: (a) In the experiment; (b) In the ABAQUS simulation; (1) Opening state (2) Transforming state (3) Closing state.

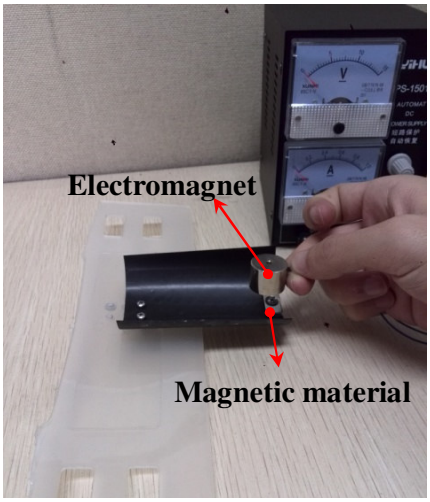

Fig. 8 Measurement of the trigger force by electromagnet.

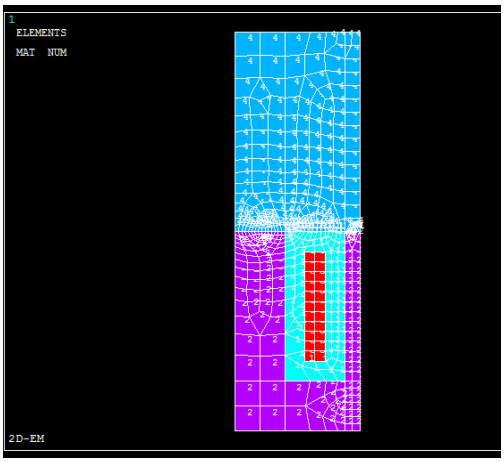

Fig. 9 Axial symmetric 2D model of the electromagnet in ANSYS software.

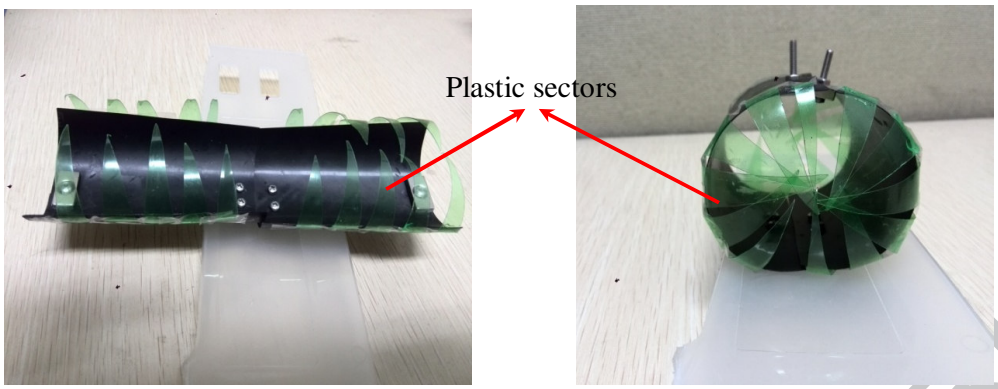

(a) (b)

Fig. 10 Venus flytrap robot with plastic sectors: (a) Opening state; (b) Closing state.

Table 1. The material properties of carbon-epoxy lamina

E_{11}(GPa)	E_{22}(GPa)	G_{12}(GPa)	G_{13}(GPa)	G_{23}(GPa)	ν_{12}	t_{ply}
105.55	7.065	5.17	5.17	5.17	0.31	0.12